arXiv:cond-mat/0601482v2 [cond-mat.str-el] 16 May 2006

Non-Fermi liquid behavior in nearly charge ordered layered metals

J. Merino[1], A. Greco[2], N. Drichko[3,4] and M. Dressel[3]
[1] *Departamento de Física Teórica de la Materia Condensada, Universidad Autónoma de Madrid, Madrid 28049, Spain*
[2] *Facultad de Ciencias Exactas Ingeniería y Agrimensura e Instituto de Física Rosario, Rosario, Argentina*
[3] *1. Physikalisches Institut, Universität Stuttgart, D-70550 Stuttgart, Germany*
[4] *Ioffe Physico-Technical Institute, 194021 St. Petersburg, Russia*
(Dated: August 13, 2013)

Non-Fermi liquid behavior is shown to occur in two-dimensional metals which are close to a charge ordering transition driven by the Coulomb repulsion. A linear temperature dependence of the scattering rate together with an increase of the electron effective mass occur above T^*, a temperature scale much smaller than the Fermi temperature. It is shown that the anomalous temperature dependence of the optical conductivity of the quasi-two-dimensional organic metal α-(BEDT-TTF)$_2M$Hg(SCN)$_4$, with M=NH$_4$ and Rb, above $T^* = 50 - 100$ K, agrees qualitatively with predictions for the electronic properties of nearly charge ordered two-dimensional metals.

PACS numbers: 71.10.Hf, 71.30.+h, 74.25.Gz, 74.70.Kn

Charge ordering phenomena appear in various strongly correlated systems such as magnetite (Fe_3O_4) [1], rare earth manganites [2], the quasi-two-dimensional organic conductors θ-, and α-(BEDT-TTF)$_2X$ [3, 4] and Na_xCO_2 [5]. The relevance of charge ordering (CO) to the superconductivity appearing in hydrated samples[6] of $Na_{0.35}CO_2$ [7] and the θ-, β''-(BEDT-TTF)$_2X$ layered organic compounds[8] has also been recently pointed out. Unconventional features observed in the optical conductivity [9] of the quasi-two-dimensional organic compounds: α-(BEDT-TTF)$_2M$Hg(SCN)$_4$ and electron Raman scattering[10] in Na_xCO_2 have been interpreted in terms of a metal close to CO. This is similar to the situation in high-T_c superconductors in which the proximity of antiferromagnetism and superconductivity has led to an intense activity in understanding the properties of metals close to an antiferromagnetic instability[11]. Anomalous metallic properties such as the opening of a pseudogap [12] and a linear temperature dependence of the resistivity [13] appear as a consequence of the development of strong short-range antiferromagnetic correlations.

In this Letter we analyze the electronic properties of metals close to a charge-order instability driven by the off-site Coulomb repulsion. We show that contributions to the single-particle self-energy due to the interaction of electrons with charge fluctuations *increase* as the temperature increases. This effect leads to effective masses increasing with temperature; opposite to the behavior expected in nearly magnetically ordered metals or in metals with strong electron-phonon interaction. This anomalous T-dependence of the effective mass is due to melting of CO with *decreasing* temperature appearing in Wigner-type transitions *i.e.* CO transitions driven by the long range part of the Coulomb repulsion. Remarkably, we find that the temperature dependence of the optical conductivity measured on α-(BEDT-TTF)$_2M$Hg(SCN)$_4$ with M=NH$_4$ and Rb above 50 K, fits qualitatively that of a two-dimensional metal close to charge-ordering.

We consider the simplest model that makes CO possible due to competition between kinetic and Coulomb energies, *i.e.* the extended Hubbard model:

$$H = \sum_{<ij>,\sigma} (t_{ij}\ c^\dagger_{i\sigma}c_{j\sigma} + h.c.) + U\sum_i n_{i\uparrow}n_{i\downarrow} + \sum_{<ij>} V_{ij}n_in_j - \mu\sum_{i\sigma} n_{i\sigma}, \quad (1)$$

which describes fermions in a lattice with an on-site Coulomb repulsion U, a nearest-neighbors Coulomb repulsion V_{ij} and a hopping matrix element t_{ij} which expresses the hopping processes between nearest-neighbors sites of the lattice. The $c^\dagger_{i\sigma}(c_{i\sigma})$ denote creation (annihilation) operators for the electron with spin σ at the i-th site, respectively, and $n_i = n_{i\uparrow} + n_{i\downarrow}$ where $n_{i\sigma} = c^\dagger_{i\sigma}c_{i\sigma}$. We assume the simplest two-dimensional case of the square lattice *i.e.* $t_{ij} = -t$ and $V_{ij} = V$ with half a hole per site (quarter filling), $n =< n_i >= 3/2$. We choose $t < 0$ which gives a hole-like Fermi surface more appropriate for the description of α and θ-type layered molecular conductors.

The ground state phase diagram of model (1) at 1/4-filling has been studied by means of Hartree-Fock [3], exact diagonalization [14], large-N Hubbard operator theory[15] and slave bosons [16]. A robust feature of the CO transition driven by V is its reentrant behavior with decreasing temperature (from a metal to a charge-ordered state back to a metal) which has been predicted by dynamical mean-field theory [17], slave boson theory[8] and finite-T Lanczos diagonalization[18]. The random phase approximation (RPA) on the extended Hubbard model[19] agrees with these approaches [20] recovering, in particular, the reentrant character of the CO transition. Little is known about the electronic properties of metals close to CO so we cover this gap by calculating the T-dependence of one-electron properties based on RPA.

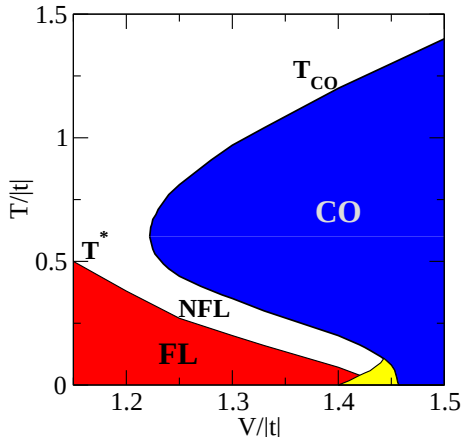


FIG. 1: (Color online) Non-Fermi liquid behavior in a metal close to charge ordering. The T-V phase diagram of the 3/4-filled extended Hubbard model for $U = 2|t|$ is shown. At $T = T_{\rm CO}$ a transition to the checkerboard charge ordered (CO) phase occurs (blue region). The low temperature scale, T^*, separates Fermi liquid (FL) behavior at low temperatures from non-Fermi liquid (NFL) above T^*. A transition to a $2\mathbf{k_F}$-CDW occurs close to CO (yellow region).

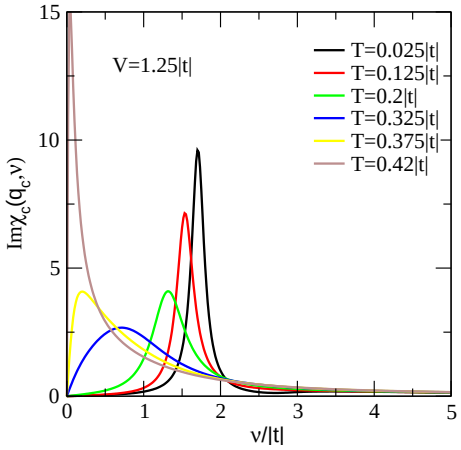


FIG. 2: (Color online) Softening of the $\mathbf{q_c} = (\pi, \pi)$ mode induced by temperature close to the charge-ordering transition for $U = 2|t|$ and $V = 1.25|t|$. It is this T-dependence of the charge susceptibility which amplifies the self-energy corrections with increasing temperature leading to anomalous thermal increase of effective masses.

The T-V phase diagram for $U = 2|t|$ plotted in Fig. 1 summarizes our main results. At $T = 0$ a transition to a $2k_F$-CDW takes place at about $V_c \approx 1.41|t|$. The temperature scale $T_{\rm CO}$ is the critical temperature for the checkerboard CO[19] transition. Non-Fermi liquid behavior occurs above T^* which evolves into conventional metallic behavior for $T < T^*$. Decreasing temperature close to the transition drives the system from a uniform metal to a CO state which transforms back to a metal as temperature is further increased. This reentrant behavior of the CO transition is responsible for the anomalous effective mass increasing with temperature above T^* as discussed below.

The reentrant behavior of the CO transition appearing in Fig. 1 can be understood from the precise form of the RPA charge susceptibility in model (1), which reads

$$\chi_c(\mathbf{q}, i\nu_n) = \frac{\chi_0(\mathbf{q}, i\nu_n)}{1 + V(\mathbf{q})\chi_0(\mathbf{q}, i\nu_n)} \qquad (2)$$

where $V(\mathbf{q}) = U/2 + 2V(\cos q_x + \cos q_y)$ (lattice spacing $a = 1$) and $\chi_0(\mathbf{q}, i\nu_n)$ is the non-interacting positive charge susceptibility which includes the two spin species and ν_n are bosonic Matsubara frequencies. Fixing $U = 2|t|$, the static charge susceptibility $\chi_c(\mathbf{q}, 0)$ diverges for $\mathbf{q} \approx 2\mathbf{k_F} = (2.4, 2.4)$ at V_c. Increasing temperature shifts the instability to $\mathbf{q_c} = (\pi, \pi)$ because then $V(\mathbf{q})$ dominates in the denominator of Eq. 2 driving the system into the checkerboard charge ordered state[19]. This leads to a softening of the $\mathbf{q}_c = (\pi, \pi)$ mode with temperature as shown in Fig. 2 where the imaginary part of the charge correlation function is plotted in the reentrant region of the transition ($V = 1.25|t|$). It is this softening induced by temperature which finally amplifies the contributions to the one-electron self-energy.

Self-energy corrections induced by temperature, at the RPA level, read:

$$\Sigma(\mathbf{k}, i\omega_n) = \frac{1}{\Omega}\sum_{\mathbf{q}} V(\mathbf{q})^2 \Big\{ \int_0^\infty \frac{\mathrm{d}\nu}{\pi} \mathrm{Im}\chi_c(\mathbf{q}, \nu) \Big[\frac{n_B(\omega') + 1 - n_F(\epsilon_{\mathbf{k}-\mathbf{q}})}{i\omega_n - \nu - \epsilon_{\mathbf{k}-\mathbf{q}}} + \frac{n_B(\omega') + n_F(\epsilon_{\mathbf{k}-\mathbf{q}})}{i\omega_n + \nu - \epsilon_{\mathbf{k}-\mathbf{q}}} \Big] \Big\}, \qquad (3)$$

with Ω being the volume. The imaginary and real parts of the self-energy, evaluated at the Fermi momentum $\mathbf{k}_F = (1.2, 1.2)$ with $U = 2|t|$ and $V = 1.25|t|$, are plotted in Fig. 3. As the temperature is increased, the imaginary part of the self-energy increases for hole propagation ($\omega < 0$) due to the coupling to the (π, π) charge fluctuating mode.

The anomalous T-dependence of the self-energy close to CO can be further explored by approximating the charge susceptibility with

$$\chi_c(\mathbf{q} \approx \mathbf{q}_c, i\omega) \approx \frac{\chi_c(\mathbf{q}_c)}{\omega_{\mathbf{q}} - i\omega}, \qquad (4)$$

with $\omega_{\mathbf{q}} = \omega_0(T) + B(\mathbf{q} - \mathbf{q}_c)^2$ and $\chi_c(\mathbf{q}_c) = \chi_c(\mathbf{q}_c, 0)$. At $T = 0$, $\omega_0(T) \to 0$ for the $\mathbf{q_c} = 2\mathbf{k_F}$-type CDW as $V \to V_c$. At finite-T, $\omega_0(T) \to 0$ as $T \to T_{\rm CO}$ signalling the CO transition at finite temperatures.

The imaginary part of the self-energy at the Fermi energy, using the approximate expression (4) is

$$\mathrm{Im}\Sigma(\mathbf{k_F}, 0) \approx \chi_c(\mathbf{q_c}) T \int_{FS} \frac{\mathrm{d}\mathbf{q}}{(2\pi)^2 |v_{\mathbf{k_F}-\mathbf{q}}|} \frac{V(\mathbf{q})^2}{\omega_{\mathbf{q}}} \arctan\left(\frac{T}{\omega_{\mathbf{q}}}\right), \qquad (5)$$

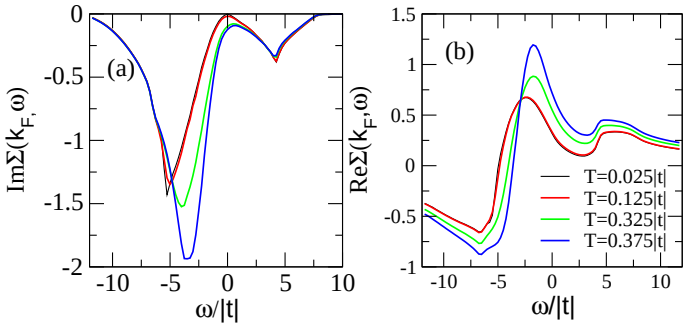


FIG. 3: (Color online) Temperature dependence of self-energy for $U = 2|t|$ and $V = 1.25|t|$. In (a) the imaginary part of the self-energy is plotted displaying the enhancement for $\omega < 0$ with temperature, while in (b) the real part shows the gradual increase of the slope at the Fermi energy above T^*.

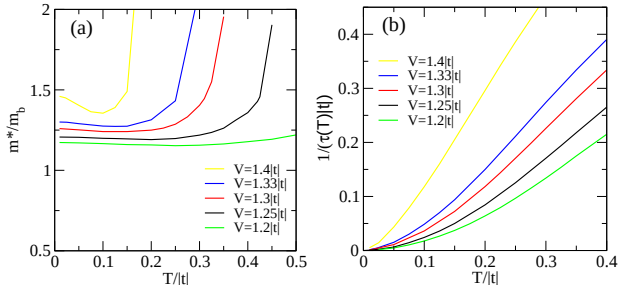


FIG. 4: (Color online) Anomalous electron effective mass enhancement induced by temperature and non-Fermi liquid behavior in a nearly charge ordered metal above T^*. In (a) the temperature dependence of the effective mass enhancement is shown for $U = 2|t|$ and different V's close to CO while in (b) the T-dependence of the scattering rate shows a linear T-dependence above T^*.

with the integration taken over momenta on the Fermi surface. Within RPA, the above expression is exact at low and high temperatures. The scattering rate exhibits Fermi-liquid behavior: $1/\tau(T) \approx A_2 T^2$, at low temperatures $T << T^*$, while at large temperatures, $T >> T^*$: $1/\tau(T) \approx A_1 T$ with the prefactors

$$A_i = \chi_c(\mathbf{q_c}) \int_{FS} \frac{d\mathbf{q}}{(2\pi)^2 |v_{\mathbf{k_F}-\mathbf{q}}|} \frac{V(\mathbf{q})^2}{\omega_{\mathbf{q}}^i}, \qquad (6)$$

which are enhanced as $V \to V_c$. The $\mathbf{q_c} = 2\mathbf{k_F}$ mode is responsible for the rapid increase in the scattering rate slope appearing in Fig. 4(b) as it connects different points at the Fermi surface giving the dominant contribution to the integration in Eq. (6). Simultaneously $T^* \to 0$ as $V \to V_c$, so the scattering rate behaves linearly down to very low temperatures close to CO.

We finally analyze the effective mass enhancement using Eq. (4) in $m^*/m_b = 1/Z = (1 - \partial \mathrm{Re}\Sigma(\mathbf{k_F}, \omega)/\partial\omega)|_{w=0}$, where m_b is the band mass. At $T = 0$, the effective mass increases as $V \to V_c$ due to the proximity to the $2\mathbf{k_F}$-CDW instability. This enhancement is $\sim \ln(1/\omega_{\mathbf{q}})$ with $\mathbf{q} \approx 2\mathbf{k_F}$ and with temperature increase below T^*, a suppression of the effective mass occurs which is $\sim (T/\omega_{\mathbf{q}})^3 \ln(T/\omega_{\mathbf{q}})$ characteristic also of nearly magnetically ordered metals[11, 21]. This behavior is more apparent in Fig. 4(a) when V is sufficiently close to V_c. However, this low temperature decrease reverses at larger temperatures *i. e.* above T^* electrons become *heavier* with temperature. This results from the softening of the $\mathbf{q} \approx (\pi, \pi)$ modes as $T \to T_{\mathrm{CO}}$ shown in Fig. 2.

In order to compare calculations with experiments on α-(BEDT-TTF)$_2M$Hg(SCN)$_4$, let us first review some of their properties. The α-(BEDT-TTF)$_2M$Hg(SCN)$_4$ compounds with M=K, Tl and Rb are quarter-filled (with holes) systems which display a density wave ground state[22] below $T_{DW} = 6 - 10$ K, whereas the M=NH4 compound is the only member of the family which exhibits superconductivity at $T_c = 1$ K. The low energy density wave state is attributed to nesting of one-dimensional sections of the Fermi surface and is rapidly degraded with temperature[23]. From our reflectivity measurements on α-(BEDT-TTF)$_2M$Hg(SCN)$_4$ compounds an analysis of the spectral weight and the width of the zero-frequency contribution of the frequency dependent conductivity yields the effective mass and scattering rate at certain temperatures [4, 24]. In Fig. 5 the experimental findings are displayed. The scattering rates for both salts show a linear temperature dependence in a broad temperature range: $T > 50 - 100$ K. Remarkably, around this temperature a change in the T-dependence of the effective mass can be also identified, showing an *increase* with temperature[25]. This crossover temperature scale is about two orders of magnitude smaller than the Fermi energy. From our theoretical predictions of a metal close to a charge-ordering transition, the linear T-dependence of the scattering rate and the increase in the effective mass occur at a very small energy scale T^* which varies between $0.14|t|$ and $0.3|t|$ for $1.25 < V/|t| < 1.33$. For typical values of the hopping matrix elements[26] for α-(BEDT-TTF)$_2M$Hg(SCN)$_4$, $t \approx 0.06$ eV, theoretical estimates yield $T^* = 0.14|t| \approx 80$ K for $V = 1.33|t|$ which is consistent with our observations[27]. Experimentally it is also found that the slope of the scattering rate of the NH_4 salt is smaller than that of Rb. From a direct comparison with our theoretical predictions (see Fig. 4) we can conclude that the Rb compound has a larger $V/|t|$ ratio than the NH_4 and is effectively closer to the charge-ordering transition. This conclusion is consistent with the comparatively larger effective mass enhancements observed for the Rb compound.

Other bosonic modes such as phonons can also lead to a linear temperature dependence in the scattering rate. In this case the crossover temperature scale set by the Debye temperature[28], $\Theta \sim 200$ K, is larger than the

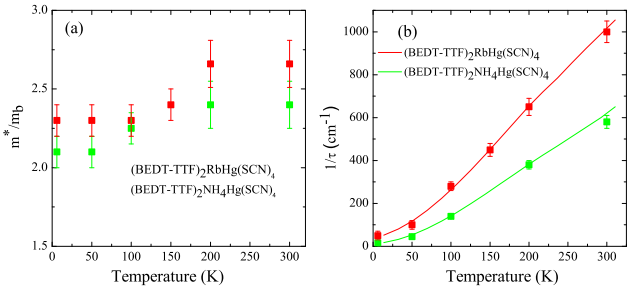


FIG. 5: (Color online) Temperature dependence of one-electron properties obtained from optical measurements on α-(BEDT-TTF)$_2M$Hg(SCN)$_4$ for the polarization parallel to the BEDT-TTF stacks. The thermal increase of effective mass enhancement (a) and the linear T-dependence of the scattering rate (b) observed above $T > T^* \approx 50 - 100$ K agrees qualitatively with RPA predictions of nearly two-dimensional charge ordered metals.

experimental T^*. It is also expected that the coupling of electrons to phonons would lead to a *suppression* of the effective mass with temperature instead of the *enhancement* experimentally observed.

In conclusion, we have shown that two-dimensional metals sufficiently close to a charge-ordering transition display non-Fermi liquid behavior including an *increase* in their electronic effective mass with temperature. The effective mass enhancement and the linear temperature dependence of the scattering rate above T^* predicted is in agreement with the optical response experimentally observed in α-(BEDT-TTF)$_2M$Hg(SCN)$_4$, indicating that they behave as nearly charge-ordered metals. Theoretical estimates of T^* are comparable with the experimentally observed value of $T^* \sim 50-100$ K, which is much smaller than the Fermi temperature. Additional probes such as angular resolved photoemission (ARPES) should be used to obtain the full temperature dependence of the electron self-energy. Strong coupling approaches should be used for determining the T-dependence of the self-energy and test the robustness of the present RPA analysis.

J. M. acknowledges financial support from the Ramón y Cajal program and MEyC under contract: CTQ2005-09385 in Spain. N.D. thanks the Alexander von Humboldt-Foundation. The experimental work was partially funded by the DFG. We acknowledge collaboration with J. Schlueter.

[1] F. Walz, J. Phys. Condens. Matter **14** 5005 (2002).
[2] S. Mori, C. H. Chen, and S. -W. Cheong, Nature (London) **392**, 473 (1998).
[3] H. Seo, J. Phys. Soc. Jpn. **69**, 805 (2002).
[4] M. Dressel and N. Drichko, Chem. Rev. **104**, 5689 (2004).
[5] Y. Wang, N. S. Rogado, R. J. Cava and N. P. Ong, Nature **423**, 425(2003).
[6] K. Takada, H. Sakurai, E. Takayama-Muromachi, F. Izumi, R. A. Dilanian, and T. Sasaki, Nature **422**, 53 (2003).
[7] O. I. Motrunich and P. A. Lee, Phys. Rev. B **70** 024514 (2005); Y. Tanaka, Y. Yanase, and M. Ogata, J. Phys. Soc. Jpn. **73**, 319 (2004).
[8] J. Merino and R. H. McKenzie, Phys. Rev. Lett. **87** 237002 (2001).
[9] M. Dressel, N. Drichko, J. Schlueter and J. Merino, Phys. Rev. Lett. **90**, 167002(2003).
[10] P. Lemmens, K. Y. Choi, V. Gnezdilov, E. Ya. Sherman, D. P. Chen, C. T. Lin, F.C. Chou, B. Keimer, cond-mat/0510756.
[11] T. Moriya, *Spin fluctuations and itinerant electron magnetism*, Springer-Verlag, Berlin, (1985).
[12] A. P. Kampf and J. R. Schrieffer, Phys. Rev. B **42** 7967 (1990); A. Kampf and J. R. Schrieffer, Phys. Rev. B **41** 6399 (1990).
[13] R. Hlubina and T. M. Rice, Phys. Rev. B **51** 9253 (1991).
[14] Y. Ohta, K. Tsutsui, W. Koshibae, and S. Maekawa, Phys. Rev. B. **50** 13594 (1994); M. Calandra, J. Merino, and R. H. McKenzie, Phys. Rev. B **66**, 195102 (2002).
[15] J. Merino, A. Greco, R. H. McKenzie and M. Calandra, Phys. Rev. B **68**, 245121(2003).
[16] R. H. McKenzie, J. Merino, J. B. Marston and O. P. Sushkov, Phys. Rev. B **64**, 085109 (2001).
[17] R. Pietig, R. Bulla and S. Blawid, Phys. Rev. Lett. **82** 4046 (1999); N. H. Tong, S. Q. Shen and R. Bulla, Phys. Rev. B, **70** 085118 (2004).
[18] C. S. Hellberg, J. Appl. Phys. **89**, 6627 (2001).
[19] A. Kobayashi, Y. Tanaka, M. Ogata and Y. Suzumura, J. Phys. Soc. Jpn. **73**, 1115 (2004).
[20] Critical temperatures, T_c, are typically overestimated by RPA. However, RPA extensions such as the fluctuating exchange approximation (FLEX) predict T_c's in good agreement with experiments[11].
[21] S. Doniach and S. Engelsberg, Phys. Rev. Lett. **17** 750 (1966); W. F. Brinkman and S. Engelsberg, Phys. Rev. B **169** 417 (1968).
[22] R. H. McKenzie, cond-mat/9706235.
[23] The Fermi surface of α-(BEDT-TTF)$_2$MHg(SCN)$_4$ contains quasi-one-dimensional sections which, if included in the calculation, would lead to similar anomalous T-dependence.
[24] N. Drichko, M. Dressel, A. Greco, J. Merino and J. Schlueter, in preparation.
[25] The effective mass increase with T above $\sim$ 50 K is a robust feature of our experimental data. However, limited accuracies inherent to the analysis prevents us to extract its precise temperature dependence.
[26] The hopping matrix element used here is appropriate for describing the quasi-1D band that crosses the Fermi energy of α-(BEDT-TTF)$_2$MHg(SCN)$_4$ with bandwidth of 0.5 eV.
[27] As $V \sim U/2$, longer range Coulomb interactions which can stabilize other Wigner-type charge ordered states different from the checkerboard, may not be negligible.
[28] R. Kondo, S. Kagoshima and M. Maesato, Phys. Rev. B **67** 134519 (2003).